Statistical Path Loss Parameter Estimation and Positioning using RSS Measurements

Henri Nurminen, Jukka Talvitie, Simo Ali-Löytty, Philipp Müller, Elena-Simona Lohan,
Robert Piché and Markku Renfors
Tampere University of Technology, Finland

Abstract

A Bayesian method for dynamical offline estimation of the position and the path loss model parameters of a wireless network's communication node is presented. Two versions of three different online positioning methods are tested using data collected from cellular networks and WLAN networks in outdoor and from WLAN networks in indoor environments. The tests show that the methods that use the estimated path loss parameter distributions with finite precisions outperform the methods that only use point estimates for the path loss parameters. They also outperform the coverage area based positioning method and path loss model method with generic path loss parameters, and are comparable in accuracy with the *k*-nearest neighbour fingerprinting method. Taking the uncertainties into account is computationally demanding, but the Gauss–Newton optimization methods is shown to provide a good approximation with computational load that is reasonable for many real-time solutions.

Keywords: indoor positioning, outdoor positioning, received signal strength, path loss model, statistical estimation

1. Introduction

Hybrid navigation means navigation using measurements from different sources, such as Global Navigation Satellite Systems (e.g. GPS), Inertial Measurement Unit, and/or local wireless networks such as cellular networks, WLAN or Bluetooth. Range, pseudorange, deltarange, altitude, map constraint and heading are examples of measurements in hybrid navigation. This paper focuses on hybrid navigation using cellular net- works and WLAN networks. The ranges from the network's communication nodes (CN) are inferred using received signal strength (RSS) measurements and path loss (PL) models.

A PL model is a model for signal attenuation in space. In the literature, for example in [1] and [2], there are many different path loss modeling methods, from deterministic and computationally heavy ray-tracing algorithms to empirical and semi-empirical channel models based on extensive measurement campaigns. Each model contains tunable parameters, which attempt to capture the nature of the investigated radio propagation environment.

The main contribution of this article is the introduction of a method for dynamic estimation of the model parameters for each CN using learning data collected at known positions. The underlying model is a simplified statistical path loss model, which omits antenna and environment factors and uses offline-estimated parameter values instead. The number of required path loss parameters is kept small in order to keep down the computational complexity and the amount of information required in the positioning phase. For example, in [3] and [4] these parameters are estimated generically for a test set of CNs, and in [5] a choice is made between several generic PL models based on the RSS value. However, the optimal parameter values are apparently CN-specific. Therefore, in this article these parameters are optimized for each CN independently. This approach has been adopted for example in [6], which only used point estimates of the estimated parameters and did not estimate their accuracy.

In this article, the estimation is based on Bayesian statistics. This is a flexible and theoretically principled framework, and there exists extensive literature on different Bayesian models and algorithms for Bayesian inference. As an important built- in property, Bayesian methods produce the statistical description of the uncertainty of estimated parameter values. Parameter precisions are needed especially if several measurements are combined e.g. in hybrid systems or in time-series filters. A Bayesian posterior distribution contains all the information provided by the measurements, so the parameter estimates can be updated with new

statistically independent measurements without needing to keep the old measurements in memory.

Furthermore, this article shows the influence of finite PL parameter precisions on the positioning results. The positioning algorithms studied here are Monte Carlo based Metropolis–Hastings (MH) sampler and computationally lighter Gauss–Newton method (GN). Grid positioning is used as a reference method. For each of the methods, two versions are compared: The first one uses point estimates for the path loss parameters and assumes them to be accurate. The second version assumes the parameters to follow specified probability distributions.

The presented methods are applicable for both cellular and WLAN networks and for both indoor and outdoor environments. Our earlier articles on those methods tested the algorithms with cellular networks in outdoor environments and with WLAN networks in indoor environments [7,8]. This article summarizes these results, also applying the methods to hybrid outdoor positioning in which both cellular and WLAN networks are involved. Static and filtering algorithms are compared. The methods are also compared with the cell-ID-based coverage area method, k-nearest neighbour method and the path loss method that assumes the path loss parameters to be common to all the CNs. Furthermore, the influence of data pruning and data aging are investigated. The performance of each method is evaluated using data sets collected from real wireless communication networks from outdoor and indoor environments, outdoor data containing both cell and WLAN measurements, and indoor data with WLAN only.

The paper is organized as follows. In Section 2 the path loss model is introduced and the method for estimating the model parameters is presented. In Section 3 a statistical measurement model for the positioning phase is presented, and the positioning algorithms are presented in Section 4. Testing and the results are described in Sections 5, 6 and 7. Finally, Section 8 presents the conclusions.

Notations: Matrices are denoted with unitalicised uppercase letters. Vectors and scalars are not distinguished. $N(m, P)$ refers to the (multivariate) normal distribution with mean m and covariance matrix P, and $N_P^m(x)$ refers to its probability density function (pdf) evaluated at x. Notation $u \leftarrow A$ means that pseudo-random number u is generated from probability distribution A.

2. Path Loss Model

2.1 Path loss model input

This section presents a method for estimating the path loss parameters and location for a single CN of a wireless network. This procedure is then applied to each CN in the learning data. The assumption that the parameters of separate CNs are statistically independent may result in some information losses, but it will simplify the form of the created CN database and reduce the number of recorded statistics.

The input for the parameter estimation procedure of a single CN is a set of RSS measurements of signals transmitted by the CN. The measurement set Ω includes N_{fp} measurements given as

$$\Omega \in \left\{ (x_i, P_i) \mid i = 1, 2, \ldots, N_{fp} \right\}, \tag{1}$$

where $x_i \in \mathbb{R}^2$ includes the easting and northing of the i:th measurement point, and P_i is the received signal power of the i:th measurement point in dBm. We assume that the transmitter power and antenna gains are fixed during the measurements, which should be a valid assumption in both WLAN and cellular networks. With this assumption, the received signal power is only dependent on the measurement coordinates x_i.

2.2 Path loss model definition

Friis's law determines the received signal power as a function of distance in a free space as

$$p_{rx}(d) = p_{tx} g_{tx} g_{rx} \left(\frac{\lambda}{4\pi d} \right), \tag{2}$$

where p_{tx}, g_{tx}, g_{rx}, and λ are the transmitted signal power, transmitter antenna gain, receiver antenna gain, and signal wavelength, respectively. The distance between transmitter and receiver antenna is d. The square term is the actual channel dependent path loss term, while the other parameters are transmitter and receiver dependent. However, using the free-space model could be a practical approach only in line-of-sight scenarios, but not in real-life cellular networks where buildings and ground surface fluctuations act as obstacles to the radio signal path.

One of the most recognized outdoor path loss models is the classical log-distance model (or power law model) [9]. In the log-distance model the received signal power is defined as

$$P_{rx}(d) = P_{rx}(d_0) - 10n \log_{10}\left(\frac{d}{d_0}\right) + w, \qquad (3)$$

where the power $P_{rx}(\cdot)$ is given in logarithmic scale, d_0 is a reference distance, n is a path loss exponent, and $w \sim N(0, \sigma^2)$ is a normally distributed random variable that models the slow fading (shadowing) effects. Here the path loss exponent n and the slow fading standard deviation depend on the local propagation environment. Notice that since the term $P_{rx}(d_0)$ indicates the received signal power at the reference distance d_0, it automatically takes into account the transmission power along with the antenna gains and wavelength shown in Eq. (2). Moreover, apart from the slow fading, $P_{rx}(d)$ is only affected by the path loss exponent n. Now, by setting $d_0 = 1$ m, and denoting $P_{rx}(d_0) = A$, it is possible to write the final path loss model as

$$P_{rx}(d) = A - 10n \log_{10}(d) + w, \qquad (4)$$

where the parameter A is referred to as the apparent transmission power.

2.3 Estimation of CN position and path loss parameters

CN position and path loss parameters are estimated using the Iterative Reweighted Least Squares method (equivalent to the Gauss–Newton method). The function to be minimized is

$$\phi(A, n, m) = \sum_{i=1}^{N_{fp}} (P - h_{est}^i(A, n, m))^2, \qquad (5)$$

$$h_{est}^i(A, n, m) = A - 10n \log_{10}\left(\|m - x_i\|\right),$$

where A is the apparent transmission power, n the path loss exponent and m the CN position. The Jacobian matrix of the vectorized measurement model function is

$$J = \begin{bmatrix} 1 & -10n \log_{10}\left(\|m - x_1\|\right) & -\frac{10}{\ln(10)} n \frac{(m - x_1)^T}{\|m - x_1\|^2} \\ \vdots & \vdots & \vdots \\ 1 & -10n \log_{10}\left(\|m - x_{N_{fp}}\|\right) & -\frac{10}{\ln(10)} n \frac{(m - x_{N_{fp}})^T}{\|m - x_{N_{fp}}\|^2} \end{bmatrix}. \quad (6)$$

The Gauss–Newton algorithm for solving the Bayesian maximum a-posteriori (MAP) estimate is described in detail in Algorithm 3.

The measurement data of cellular networks tends to be spatially correlated [10]. In order to reduce the effect of correlations, the measurements are pooled on a grid of pre-specified points before the estimation process. The RSS value of a grid point is the mean of the RSSs observed in the grid point's neighbourhood. The distance of adjacent grid points was set to 50 m for outdoor and 5 m for indoor environments.

To improve convergence properties of the Gauss–Newton algorithm, all the quantities are given an almost uninformative Gaussian prior, i.e. a Gaussian distribution with so large a variance that the prior's influence on the posterior mode is negligible. The initial value for the CN position in the iterative solution is the position of the strongest measurement, to help ensure that the algorithm does not get trapped at a local extremum in an area of weak RSSs. Initial values for A and n can be chosen more arbitrarily from the valid ranges, since the distribution is typically unimodal when the number of data points is large.

The algorithm also returns an approximation for the covariance matrix of each quantity. Consequently, we are potentially able to distinguish between trustworthy and untrustworthy path loss models. In the Bayesian sense, the algorithm tries to estimate the MAP value and the covariance matrix is the covariance of the linearized model.

In an ideal case without any slow fading variations, the CN position would be found at the coordinate point where the received signal power reaches its maximum value. However, in practice there might be several clear peaks in the received signal power map or there might not be enough measurements to find even a single peak. Besides, the CN might not even be located inside the measured power map.

However, it should be emphasized that there is no need to know the exact true CN positions as long as the same estimated CN positions are used also in the positioning phase. Thus, one could easily refer to a certain kind of pseudo CN positions. Furthermore, it can be shown that using correct CN positions may even result in a worse modeling outcome. One reason is that the used 2D model does not work accurately in close proximity of the CN position where CN antenna height and antenna tilting have a considerable effect on the received signal power.

2D-projection effects are taken into account by modifying the covariance matrix of the CN position artificially by adding a constant to elements on the diagonal. This modification models also the effects of GPS errors in the learning data and measurement error correlations due to environmental effects. For this reason and for reducing the number of recorded parameters, the CN positions and path loss parameters are assumed to be uncorrelated. Fig. 1 shows power maps (interpolated between the measurement points) of two separate CNs
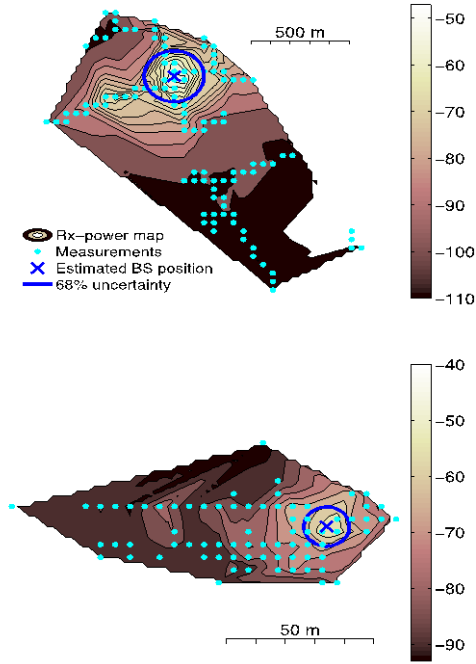
Figure 1: Power maps and estimated CN positions of a WCDMA cell (up) and a WLAN access point
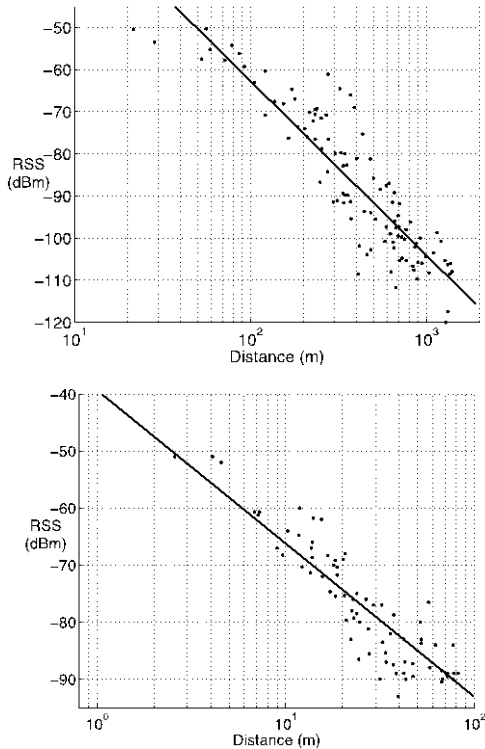

Figure 2: Path loss curves of a WCDMA cell (up) and a WLAN access point

and the resulting CN position estimates along with the covariance ellipse.

As pointed out before, the path loss exponent n and the slow fading standard deviation are highly dependent on the radio propagation environment. For example, in a shadowed urban cellular radio network the typical values of n and σ are varying around 0.1–4 and 1–6 dB, respectively [2,11]. Examples of path loss model curves can be found in Fig. 2, in which the path loss models are derived for the same CNs that were previously show in Fig. 1.

3.   Estimation Theory

3.1 Bayesian filtering equations
Consider the Gaussian system

$$\begin{aligned}
x_{k+1} &= \Phi x_k + w_k \\
y_k &= h(x_k, a) + v_k
\end{aligned}, \qquad (7)$$

where y_k is the vector of observations at time instant t_k, x_k represents the state of the system at t_k and a represents nuisance parameters that have prior distribution $p(a)$. The motion model is linear and independent of the nuisance parameters. The random noise terms $w_k \sim N(0, Q_k)$ and $v_k \sim N(0, R_k)$ are assumed to be mutually independent and independent of the state x and the parameter vector a. Matrix Φ is the state transition matrix.

By the Chapman–Kolmogorov equation, the prior distribution of the state at time instant k is

$$p(x_k | y_{1:k-1}) = \int p(x_k | x_{k-1}) p(x_{k-1} | y_{1:k-1}) dx_{k-1}. \qquad (8)$$

This is the prediction step of a Bayesian filter. It is assumes that the estimate of parameter vector a is not modified online, so it is approximated that the distribution of a remains unaffected by the data that is received in the positioning phase, i.e. $p(a | x_{1:k}, y_{1:k}) \approx p(a)$. By Bayes' rule, the posterior pdf of the state is thus

$$\begin{aligned}
p(x_k | y_{1:k}) &= \int p(x_k, a | y_{1:k}) da \\
&= \frac{\int p(y_k | x_k, a) p(x_k, a | y_{1:k-1}) da}{\int \int p(y_k | x_k, a) p(x_k, a | y_{1:k-1}) da\, dx_k} \\
&\approx \frac{\int p(y_k | x_k, a) p(a) p(x_k | y_{1:k-1}) da}{\int \int p(y_k | x_k, a) p(a) p(x_k | y_{1:k-1}) da\, dx_k}
\end{aligned} \qquad (9)$$

This is the update step of the Bayesian filter with unknown static nuisance parameters in the measurement model.

The filtering technique used in this article is an approximation of the general Bayesian filtering procedure described above. The presented positioning algorithms are formulated so that they return the posterior mean x_k^+ and covariance matrix Σ_k^+ of the user position. The posterior distribution is then approximated by a normal distribution with the estimated parameter values. Using this simplification and linear motion model with additive Gaussian noise, the filter prediction step (8) becomes

$$p(x_k \mid y_{1:k-1}) = N_{\Phi\Sigma_{k-1}^+\Phi^T+Q}^{\Phi x_{k-1}^+}(x_k), \qquad (10)$$

where

$$\Phi = I_{2\times2}, \quad Q \propto (\Delta t)^2 \cdot I_{2\times2}.$$

This approximation is done in order to simplify the prediction step of the filter, which is now the conventional Kalman filter prediction. Note that this procedure may result in information losses especially in case of multimodal posterior. Finding the optimal scaling of the process noise covariance matrix Q may be problematic since it depends on the user's movement patterns. In the tests of this article the value was tuned for indoor and outdoor tracks separately.

3.2 Path loss model

The path loss model with uncertain parameters presented in Section 2 is a special case of the observation model in (7). In this case, $y_k = \begin{bmatrix} P_1 & \cdots & P_{N_P} \end{bmatrix}^T$ is the vector of N_P RSS measurements from different CNs at time instant t_k and x_k is the user position. Parameter vector a contains the path loss model parameters of all the possible CNs:

$$a = \begin{bmatrix} A_1 & n_1 & m_1^T & \square & A_{N_P} & n_{N_P} & m_{N_P}^T \end{bmatrix}^T.$$

The PL models are not updated online, so the approximation (9) is used. The measurement model function is

$$h(x,a) = \begin{bmatrix} A_1 - 10n_1 \log_{10}(\|m_1 - x\|) \\ \vdots \\ A_{N_P} - 10n_{N_P} \log_{10}(\|m_{N_P} - x\|) \end{bmatrix}.$$

Measurement noise covariance matrix is $R = \sigma^2 \cdot I_{N_P \times N_P}$.

The PL parameter's distributions are modelled to be normal, since the Gauss–Newton algorithm requires this in its basic form and the normal pdf of A and n is the conjugate prior of the likelihood. However, other distribution families such as Student's t-distribution could also be studied. For simplicity, it is also assumed that CN position and PL parameters are independent a priori. Thus,

$$p(a) = p(A_{1:N_P}, n_{1:N_P}, m_{1:N_P})$$
$$= \prod_{i=1}^{N_P} N_{\Sigma_{A_i,n_i}}^{\mu_{A_i,n_i}} \left(\begin{bmatrix} A_i \\ n_i \end{bmatrix} \right) \cdot N_{\Sigma_{m_i}}^{\mu_{m_i}}(m_i), \qquad (11)$$

where the parameters $\mu_{A_i,n_i} = \begin{bmatrix} \mu_{A_i} & \mu_{n_i} \end{bmatrix}^T$, Σ_{A_i,n_i}, μ_{m_i} and Σ_{m_i} are estimated from the learning data using the Gauss–Newton algorithm of Section 2.3.

4. Positioning Algorithms

In this section a Gaussian prior distribution $p(x) = N_{\Sigma}^{x^-}(x)$ is used for the user's position. In case of multimodal likelihood function, the prior may function as a regularizer. Furthermore, it may reflect location information from other sources, and in case of time series filtering, the filter's prediction distribution is the prior.

4.1 Grid method

By (9) the posterior pdf value at point x is

$$p(x \mid P_{1:N_P}) \propto \prod_{i=1}^{N_P} \iiint p(P_i \mid x, A_i, n_i, m_i) p(A_i, n_i) p(m_i)$$
$$dA_i dn_i dm_i \cdot p(x), \qquad (12)$$

which can be approximated using standard Monte Carlo integration. The grid method is presented in Algorithm 1.

The most crucial implementation issues are the Monte Carlo sample size parameter N as well as grid size and density. Note that CN likelihoods are combined using logarithms to avoid numerical underflows.

4.2 Metropolis–Hastings method

The Metropolis–Hastings (MH) sampler generates Monte Carlo samples from an arbitrary posterior distribution of a multivariate random variable. It is an iterative algorithm that can be proved to converge under mild restrictions towards the target distribution as the Monte Carlo sample size increases. The posterior mean and covariance can then be approximated by the sample mean and covariance of the sampled set. The algorithm is presented in Algorithm 2.

Algorithm 1 Grid with Monte Carlo integration

1. Set a grid $\{x_m \in \mathbb{R}^2 \mid m \in \{1,...,N_m\}\}$ that covers most of the prior probability mass.

2. For each observed CN $i = 1,...,N_P$, draw

$$\begin{bmatrix} A_i^{(k)} \\ n_i^{(k)} \end{bmatrix} \leftarrow N\left(\begin{bmatrix} \mu_{A_i} \\ \mu_{n_i} \end{bmatrix}, \Sigma_{A_i,n_i} \right)$$

$$m_i^{(k)} \leftarrow N\left(\mu_{m_i}, \Sigma_{m_i} \right)$$

for $k = 1,...,N$.

3. At each grid point x_m compute for each CN $i = 1,...,N_P$ and for each sample $k = 1,...,N$

$$I_{i,m}^{(k)} := N_{\sigma^2}^{P_i}\left(A_i^{(k)} - 10 n_i^{(k)} \log_{10}\left(\left\| m_i^{(k)} - x_m \right\| \right) \right),$$

and $I_{i,m} := \frac{1}{N}\sum_{k=1}^{N} I_{i,m}^{(k)}$. Then set

$$\ell_m := \ln\left(N_{\Sigma^x}^{x}(x_m) \right) + \sum_{i=1}^{N_P} \ln(I_{i,m}), \quad L_m := \exp(\ell_m).$$

4. Normalize the grid to get a set of weights $w_m = \frac{L_m}{\sum_{m=1}^{N_m} L_m}$ and compute mean and covariance estimates

$$x^+ := \sum_{m=1}^{N_m} w_m x_m, \quad \Sigma^+ := \sum_{m=1}^{N_m} w_m\left(x_m - x^+ \right)\left(x_m - x^+ \right)^T.$$

The MH sampler uses a so-called proposal distribution, from which it is straightforward to generate random numbers. At each iteration of the algorithm, proposal values for the estimated variables are drawn from the proposal distribution. The proposal values are then accepted with probability proportional to the ratio of the pdf values of the proposal value and the latest accepted value. [12, Ch. 5]

It can be proved that

$$p(x, m_{1:N_P} \mid P_{1:N_P})$$

$$\overset{(9)}{\propto} \iint p(P_{1:N_P} \mid x, A_{1:N_P}, n_{1:N_P}, m_{1:N_P}) \cdot p(A_{1:N_P}, n_{1:N_P})$$

$$dA_{1:N_P} dn_{1:N_P} \cdot p(x) \cdot p(m_{1:N_P}) \tag{13}$$

$$\propto p(x) \prod_{i=1}^{N_P} p(m_i) \det(S_i)^{\frac{1}{2}} \exp\left(\tfrac{1}{2} z_i^T S_i^{-1} z_i \right)$$

where

$$S_i := \left(\tfrac{1}{\sigma^2} B_i^T B_i + \Sigma_{A_i,n_i}^{-1} \right)^{-1}, \quad z_i := S_i\left(\tfrac{1}{\sigma^2} B_i^T P_i + \Sigma_{A_i,n_i}^{-1} \begin{bmatrix} \mu_{A_i} \\ \mu_{n_i} \end{bmatrix} \right),$$

with $B_i = \begin{bmatrix} 1 & -10\log_{10}(\|m_i - x\|) \end{bmatrix}$. The simple form of this formula enables analytical integration over PL parameters A and n.

In the implementation phase, great care must be taken when setting the proposal distributions to ensure the algorithm's convergence in a feasible number of iterations. For convenience, the proposal distributions are chosen to be multivariate normal with the latest accepted value as the mean and the covariance matrices P_x and P_{m_i} tuned from prior covariance matrices of x and $m_{1:N_P}$.

Algorithm 2 Metropolis–Hastings algorithm

1. Set $x^{(0)} := x^-$, $A_i^{(0)} := \mu_{A_i}$, $n_i^{(0)} := \mu_{n_i}$ and $m_i^{(0)} := \mu_{m_i}$ for $i = 1,...,N_P$. Set $p^{(0)}$ using the formulas in step 3. Set $k := 1$.

2. Generate $x'^{(k)} \leftarrow N\left(x^{(k-1)}, P_x \right)$, and for each CN $i = 1,...,N_P$, generate $m_i'^{(k)} \leftarrow N\left(m_i^{(k)}, P_{m_i} \right)$.

3. For each $i = 1,...,N_P$, compute

$$B_i^{(k)} := \begin{bmatrix} 1 & -10\log_{10}\left(\left\| m_i'^{(k)} - x_i'^{(k)} \right\| \right) \end{bmatrix} \text{ and}$$

$$S_i^{(k)} := \left(\tfrac{1}{\sigma^2} B_i^{(k)T} B_i^{(k)} + \Sigma_{A_i,n_i}^{-1} \right)^{-1}$$

$$z_i^{(k)} := S_i^{(k)}\left(\tfrac{1}{\sigma^2} B_i^{(k)T} P_i + \Sigma_{A_i,n_i}^{-1} \begin{bmatrix} \mu_{A_i} \\ \mu_{n_i} \end{bmatrix} \right).$$

Set

$$p'^{(k)} := \ln\left(N_{\Sigma^x}^{x}\left(x'^{(k)} \right) \right) + \sum_{i=1}^{N_P}\left[\tfrac{1}{2}\ln\left(\det\left(S_i^{(k)} \right) \right) \right.$$

$$\left. + \tfrac{1}{2} z_i^{(k)T} S_i^{(k)-1} z_i^{(k)} + \ln\left(N_{\Sigma_{m_i}}^{\mu_{m_i}}\left(m_i'^{(k)} \right) \right) \right].$$

4. Set $x^+ := \frac{1}{N}\sum_{k=1}^{N} x^{(k)}$ and $r := \exp\left(p'^{(k)} - p^{(k-1)} \right)$.

   Generate $u \leftarrow \text{Uni}(0,1)$. Compute

   if $r > u$ **then**
       for $i = 1:N_P$ **do**
           $m_i^{(k)} := m_i'^{(k)}$
       end for
       $x^{(k)} := x'^{(k)}$, $p^{(k)} := p'^{(k)}$
   else
       for $i = 1:N_P$ **do**
           $m_i^{(k)} := m_i^{(k-1)}$
       end for
       $x^{(k)} := x^{(k-1)}$, $p^{(k)} := p^{(k-1)}$
   end if

5. Set $k := k+1$. If $k < N$, go to step 2. Otherwise, set

$$x^+ := \frac{1}{N}\sum_{k=1}^{N} x^{(k)}, \quad \Sigma^+ := \frac{1}{N}\sum_{k=1}^{N}\left(x^{(k)} - x^+ \right)\left(x^{(k)} - x^+ \right)^T.$$

4.3 Gauss–Newton method

With suitable measurement models, iterative state estimation methods can be as accurate as any closed form solution but simpler and easier to implement [13]. The Gauss–Newton method, also known as the Iterative Reweighted Least Squares method, is tested for positioning with the presented path loss model. The detailed description is in Algorithm 3.

The iteration is not guaranteed to converge globally, but including good enough prior information and initial values seems to prevent the method from diverging. To improve convergence properties further, the step length in the state-space is chosen by a simple line search method so that the objective function value decreases at every iteration. However, the number of line search iterations is limited to ensure stability. The global convergence properties of the Gauss–Newton method with damped step size are discussed in [14,15].

For formulating the Jacobian matrix that is needed in the Gauss–Newton algorithm, the analytical partial derivatives of the measurement function h are formed:

$$\frac{\partial h_i}{\partial x} = \frac{10}{\ln(10)} n_i \frac{(m_i - x)^T}{\|m_i - x\|^2}, \ \frac{\partial h_i}{\partial A_i} = 1,$$

$$\frac{\partial h_i}{\partial n_i} = -10 \log_{10}(\|m_i - x\|), \ \frac{\partial h_i}{\partial m_i} = -\frac{10}{\ln(10)} n_i \frac{(m_i - x)^T}{\|m_i - x\|^2}.$$

The remaining partial derivatives are zeros. Note that the prior covariance matrix is always full rank, so the least-squares estimation can be performed. The measurement covariance matrix $\mathbf{R}$ is the diagonal matrix of the measurement variances. In Algorithm 3 the complete state is denoted with $z = \begin{bmatrix} x \\ a \end{bmatrix}$. As in the PL parameter estimation phase, the output of the algorithm contains estimates for the MAP and the covariance matrix of the posterior of the linearized model.

4.4 Comparison methods

The presented methods are compared with two conventional positioning methods: in indoor and outdoor cases with statistical coverage areas (CA) [16,17] and in indoor cases with the (weighted) *k*-nearest neighbour algorithm (WKNN) [18]. The statistical CAs are bivariate Gaussian distributions that are fitted to the fingerprint database. Since the product of Gaussian densities is a Gaussian density, the standard Kalman filter can be applied to these measurements. In the WKNN method, the measurements are not compressed into parametric form, i.e. no statistical assumptions are made of the measurement model. Instead, the whole

---

Algorithm 3 Gauss–Newton algorithm

1. Choose the stopping tolerance δ. Let

    $$\Sigma_z := \text{blkdiag}\left(\Sigma^+, \Sigma_{A_1, n_1}, \Sigma_{m_1}, ..., \Sigma_{A_{N_p}, n_{N_p}}, \Sigma_{m_{N_p}}\right)$$

    and

    $$z^- := \begin{bmatrix} x^{-T} & \mu_{A_1} & \mu_{n_1} & \mu_{m_1}^T & \cdots & \mu_{A_{N_p}} & \mu_{n_{N_p}} & \mu_{m_{N_p}}^T \end{bmatrix}$$

    be the prior covariance and mean. Let the initial iterand be $z_0 := z^-$. Additionally, measurement variance σ^2 is required. Set $k := 0$. Denote the objective function with

    $$\theta(z) := \left(z - z^-\right)^T \Sigma_z^{-1}\left(z - z^-\right) + \frac{1}{\sigma^2} \sum_{i=1}^{N_P} (h_i(z) - P_i)^2.$$

2. Compute the Jacobian

    $$\mathbf{J}_k := \begin{bmatrix} \frac{\partial h_1}{\partial x} & \frac{\partial h_1}{\partial A_1} & \frac{\partial h_1}{\partial n_1} & \frac{\partial h_1}{\partial m_1} & \mathbf{0}_{4(N_P - 1)}^T \\ \vdots & & \ddots & & \vdots \\ \frac{\partial h_{N_P}}{\partial x} & \mathbf{0}_{4(N_P - 1)}^T & \frac{\partial h_{N_P}}{\partial A_{N_P}} & \frac{\partial h_{N_P}}{\partial m_{N_P}} & \frac{\partial h_{N_P}}{\partial m_{N_P}} \end{bmatrix}.$$

3. Set

    $$\Delta z_k := -\left(\Sigma_z^{-1} + \frac{1}{\sigma^2} J_k^T J_k\right)^{-1}$$
    $$\cdot \left(\Sigma_z^{-1}(z_k - \mu_z) + \frac{1}{\sigma^2} J^T \left(h(z_k) - P\right)\right).$$

4. Choose the step length:
    $$\alpha := 1$$
    while $\left\|\theta(z_k + \alpha \Delta z_k)\right\| \geq \left\|\theta(z_k)\right\|$ **and** $\alpha > \alpha_0$ **do**
    $$\alpha := \frac{\alpha}{2}$$
    end while
    where α_0 is a configuration parameter, e.g. 0.05. Set $z_{k+1} := z_k + \alpha \cdot \Delta z_k$.

5. If stopping condition $\left\|\Delta z_k\right\| < \delta$ is not satisfied and $k \leq k_{\max}$, increment k and repeat from Step 2. Otherwise, compute $\mathbf{P} := \left(\Sigma_z^{-1} + \frac{1}{\sigma^2} J_k^T J_k\right)^{-1}$ and set the state estimate
    $$x^+ := z_{k+1, 1:2}, \ \Sigma^+ := \mathbf{P}_{1:2, 1:2}.$$

---

measurement database is stored in the memory. In the positioning phase, the difference of the measurement to each database point is computed using the Euclidean distance of RSS differences, and the location estimate is set to the mean value of the three closest database points. The CNs that were observed in the positioning phase but that do not appear in a learning data point are taken into account in RSS-distance calculation by using –120 dBm as a radiomap value. The WKNN estimates are not filtered in this paper, so the algorithm only uses measurements of the current time instant.
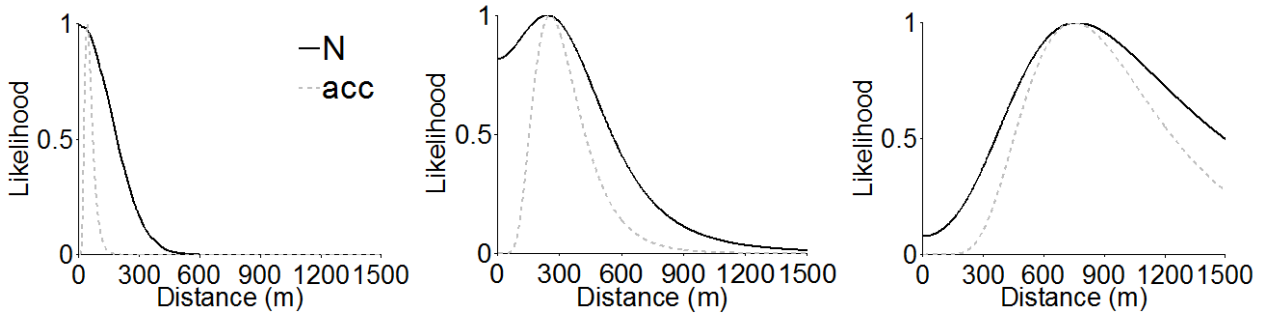
Figure 4: Likelihoods of measurements –50, –75 and –90 dBm as a function of the distance from the mean of the CN position estimate. Curve "N" represents algorithms that assume PL parameters to be normally distributed *a priori,* and curve "acc" the algorithm that assumes that the parameters are known accurately.

5.   Likelihood Illustrations

Fig. 3 illustrates the influence of the uncertain parameters on the likelihood. In the presented case $\begin{bmatrix} A \\ n \end{bmatrix} \sim N\left(\begin{bmatrix} 2 \\ 3.2 \end{bmatrix}, \begin{bmatrix} 100 & 3.5 \\ 3.5 & 0.15 \end{bmatrix} \right)$ and $m \sim N\left(0, 2 \cdot 10^4 \cdot I \right)$. These representative values are based on our experimental knowledge of the Finnish cellular network. The likelihoods are calculated using the grid algorithm. The upper row illustrates the likelihoods of the model that takes the parameter uncertainties into account, and the lower row shows the likelihoods when it is assumed that the path loss parameter values are correct. The RSS values corresponding to the likelihoods are -50 (on the left), -75 and -90 dBm. The path loss model standard deviation is $\sigma = 6$ dB. It can be seen that with strong signals, the RSS likelihood is unimodal or almost unimodal when the parameter uncertainties are taken into account.

In the case of radially symmetric CN position distribution, the posterior density depends only on the distance from the mean of the CN position estimate. Fig. 4 illustrates the likelihoods of the user's position as a function of this distance. They have been computed using standard Monte Carlo integration and normalized so that the maximal likelihood value is one. Curve "N" represents algorithms that assume PL parameters to be normally distributed *a priori*, and curve "acc" the algorithms that assume that the parameters are known accurately. Fig. 4 shows that the tails of the "N" curve are considerably heavier.

In Fig. 5 the likelihood of two RSS measurements of –80 dBm is presented. The PL parameters are similar to the ones in Fig. 3, and the distance between CNs is 400 meters. If the parameter uncertainties are not taken into account (the figure on the right), the support of the likelihood consists of two separate parts, whereas in the left figure there is significant amount of likelihood mass also in the CN positions' surroundings.

Figure 3: The likelihoods of measurements –50, –75 and –90 dBm. In the upper row, parameter uncertainties have been taken into account.
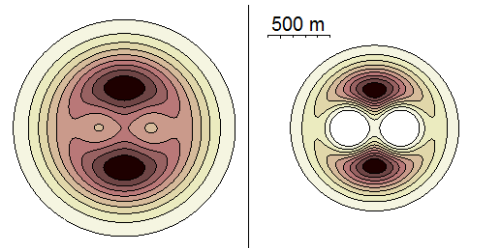
Figure 5: The combined likelihood of two CNs with signal strengths –80 dBm. On the left, parameter uncertainties have been taken into account.

6.   Outdoor Tests

6.1 Experiment setup

A measurement campaign was accomplished to evaluate the performance of different algorithms in a real use case. First, a large set of outdoor fingerprints was collected in Tampere, Finland for learning the radiomap. The measurement device was a mobile phone with a suitable logging software and GPS receiver. The data contains IDs of both observed WCDMA cellular base stations (BS) and WLAN access points (AP). The measured RSS values are based on the measured

Received Signal Code Power (RSCP) indicator reported by the user equipment.

In this article, two separate outdoor test tracks are presented. The first track (Hervanta) was collected by a pedestrian in a densely populated urban/suburban area. In the second track (Lukonmäki) the measurer rode a bicycle with a low velocity in a suburban area. In all the cases the true user positions were tracked using conventional GPS positioning. By plotting the GPS solutions on the map, it was confirmed that the GPS error on the area is small compared to the cellular positioning accuracy. The measurement interval was approximately 1 second, but the measurements were used for estimation with ten seconds interval to reduce measurement error correlations and to simulate the real use-case in which power should be saved.

The coverage area (CA) of each BS and AP was estimated by fitting a normal distribution to the data [16,17]. Furthermore, path loss model parameters were estimated using the method of Section 2 of this article. In the static positioning, the prior distribution for the user's position was the product of CAs. In time-series filtering, the prior was the product of the filter prediction and the CA estimate.

6.2 Parameter estimation results

Fig. 6 shows the distribution of the estimates of the PL parameters A and n and BS positions m which were obtained from the collected data. The plots show the empirical quantiles of the means and standard deviations of the parameters. The distribution of the correlation coefficients, that is, the ratio of the covariance and product of standard deviations of A and n, is also shown.

Fig. 6 indicates that there is broad variation in the values of the PL parameters A and n. Furthermore, at least 10 % of the BSs has very high parameter variances for A or n or both compared to the majority of the BSs. The PL parameters are in majority of the cases highly correlated. The correlation coefficient is always positive, since increasing the y-intercept term of the fitted line A always makes the slope $-n$ more negative.

6.3 Positioning results with static and filtering algorithms

The positioning results of the real-data outdoor tests are in Tables 1 and 2 for the static and filtering algorithms respectively. In the filter, the prediction step is the Kalman prediction based on equation (10) and the update step is one of the positioning algorithms 1, 2 or 3. Abbreviation "N" stands for the algorithms that assume the path loss parameters to be normally distributed a priori whereas "acc" indicates that the parameter values
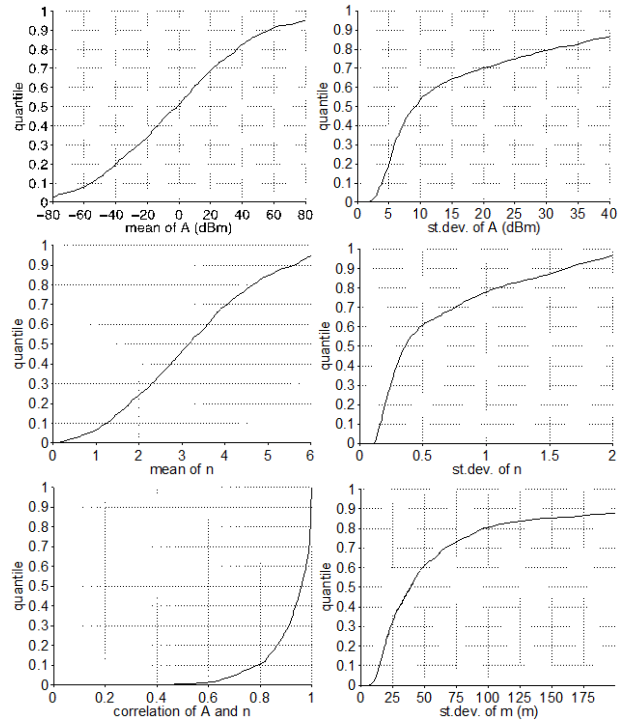
Figure 6: Estimate distributions for outdoor cellular BSs: means of A (up left), standard deviations of A (up right), means of n (middle left), standard deviations of n (middle right), correlation coefficients of A and n (low left), and square-rooted maximal eigenvalues of the covariance matrices of m (low right)

are assumed accurate. "CA" refers to the method in which only the product of coverage areas is used. Note that the performance of the filter is highly dependent on the process noise coefficient in (10). The chosen value of this parameter was a compromise between the optima of different tracks.

For evaluating the performance of the algorithms we rely on statistics of positioning errors. The positioning error at one time step is the Euclidean distance between the position estimate and the corresponding reference location. Columns "Mean", "Med" and "95 % err." in the tables are mean error, median error and empirical 95 % percentile of errors in meters. "Time" is the average running time of our MATLAB implementation in seconds. Note that the codes are not highly optimized so the running time values have to be considered only roughly indicative. The times are also highly dependent on the chosen configuration parameters.

Column "Cons" displays the 95 % consistency that is determined using the Gaussian consistency test [19, p. 235] with risk level 5 %. The solver is deemed to be consistent at a certain time step, if the true position is within the 95 % ellipse of the posterior distribution, assuming normality of the posterior. For the case of

Gaussian posterior distribution, the closer "Cons" is to 95 %, the more realistic the covariance matrix estimation is. Note that in the case of RSS measurements the true posterior cannot be expected to be Gaussian, and the validity of the consistency test may suffer in multimodal and heavy-tailed cases. These cases occur especially if the prior has large variance and the number of measurements is low.

From Table 1 it can be seen that taking the parameter uncertainties into account improves the consistency remarkably for all the estimation methods. Accurate covariance matrix estimation is crucial especially when location information from other sources is combined with RSS measurements or when positioning is done with Bayesian time-series filters [20].

The presented "N" algorithms seem to outperform "acc" algorithms slightly in the positioning accuracy. In the Hervanta case, time-series filtering reduces mean errors by at least 10 %, and performance differences between "N" and "acc" algorithms are somewhat clearer than in the static results. For the Lukonmäki case, the performance improvement of the filter compared to the static algorithms is not as clear as in Hervanta, except in 95 % error. This indicates that the data quality in Lukonmäki is most of the time so good that filtering does not provide significant improvement, but it mainly helps in difficult cases where the number of observed cells is low or the measurements are noisy. Both the GPS solution and the estimated track of the Lukonmäki case are plotted on the map in Figure 7. These figures illustrate the filtering algorithm's tendency to make the appearance of the estimated track smoother and less jumpy.
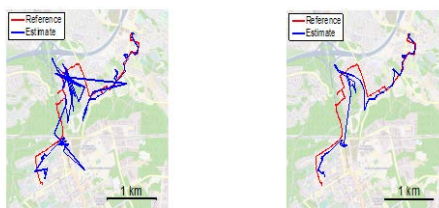

Figure 7: The GPS track (Reference) and the track estimated by the Gauss–Newton algorithm (Estimate) for the Lukonmäki test track. The static solution is on the left, and the filtering solution on the right. (The map is © openstreetmap.org contributors.)

Among the three estimation methods, the grid and MH sampler approach the exact Bayesian posterior distribution. The grid gives the precise posterior values in the grid points assuming that the Monte Carlo integration's accuracy is adequate. The MH sampler converges theoretically to the true posterior as the sample size parameter N approaches infinity. In practice,

the rate of convergence in MH algorithms is highly dependent on the form and parameters of the proposal distributions. With the chosen configuration the method usually fails to compete with the grid especially in consistency. However, the Monte Carlo framework is a flexible and efficient tool especially in time-series analysis of highly nonlinear or non-Gaussian measurements [21].

The Gauss–Newton method lacks global convergence properties and the covariance matrix estimate is based on a linearized model and has thus a less clear Bayesian interpretation. Indeed, the real data tests show that the algorithm's convergence is more sensitive to the quality of the prior distribution. However, the presented results are comparable with those of the other methods, and the GN is clearly the computationally lightest one of the presented PL algorithms.

6.4 Positioning results using pruned learning data
In the middle column of Table 2 the learning data set was pruned so that for 75 % of the BSs only 10 % of the data points were used for parameter estimation. The excluded points were chosen randomly. This models a real use case, since there might be newly added BSs or the area as a whole might be inadequately covered by the database.

Based on the obtained results the positioning errors with the pruned data are approximately 10 % higher than those with the complete data set. In the Lukonmäki case the results are even slightly better in median error sense with the pruned learning data, but in the 95 % sense worse, which might indicate that pruning results in an increase in the number of outlier measurements. It also seems that pruning tends to amplify slightly the performance differences of "N" and "acc" algorithms. Theoretically it is obvious that PL parameter uncertainties should be taken into account especially if some of the BSs are likely to be badly mapped, since the parameter uncertainties' function is to compare the reliabilities of different BSs' PL models.

6.5 Positioning results using generic parameters
The right column of Table 2 presents the positioning results of the same test tracks obtained using generic PL model parameters. In this approach the Gauss–Newton parameter estimation method of Section 2 is applied to the whole learning data set, and the estimated parameters are BS position for each BS and PL parameters A and n that are common for all the BSs. Coverage areas are also estimated for each BS separately.

In the Hervanta case the generic parameters seem to increase the errors by at least 25 % compared to the results obtained with BS-specific PL parameters, whereas in the Lukonmäki case the error statistics are

rather similar. The generic parameters approach is more efficient in terms of data storage, but loses BS-specific environment information.

6.6 Positioning results using combined cell and WLAN

Table 3 presents the corresponding positioning results from the Lukonmäki track obtained so that the information contained by the received WLAN signals is fused to the cellular positioning estimate. The PL parameters and CN positions of the WLAN APs were estimated using the same learning data as with cellular BSs, but without the pre-specified grid. In the left part of the Table 3 the used WLAN information is the CAs of the WLAN APs, in the middle part the WLAN CAs and RSSs and in the right table the RSS measurements of WLANs. In each case both cell CAs and cell RSSs are also used.

The results indicate that WLAN RSS measurements do not contain any additional position information in outdoor cases compared to mere connectivity information of WLANs (CAs). However, the WLAN CA methods seem to underestimate the uncertainty in the position estimate, which is indicated by the low 95 % consistencies. The reason for this behaviour is a topic for future research.

7. Indoor Tests

7.1 Experiment setup

A large set of WLAN fingerprints was collected in public indoor spaces in the city of Tampere, Finland for learning the radiomap. The test case presented in this article is located in a building at Tampere University of Technology campus area. The test track consists of several parts measured on different floors of the same building. Each floor has a separate radiomap with 2-dimensional PL models, and the correct floor is assumed known in both learning and positioning phases. Suitable floor detection methods are under research.

The measurement device was a tablet computer. The reference locations were set manually on the floor plan figure. The WLAN scanning interval was varying between 10 s and 20 s.

7.2 Results and discussion

The distributions of the PL parameter and AP position estimates and their standard deviations are presented in Fig. 8. It is also clearly visible in the indoor WLAN data

that the PL parameters are not global constants but have significant variation over different APs.

The error statistics of the real-data indoor tests are in Table 4 and Table 5. In the middle column of Table 4 only randomly chosen 10 % of the fingerprints in the learning data were used for randomly chosen 75 % of the APs, and in the right column the PL parameters A and n were assumed to be generic for all the APs. The results of Table 5 are based on the same radiomap and covers approximately the same positioning tracks as the other tests, but the positioning track data were collected one and a half years later. Abbreviation "N" stands for the algorithms that assume the PL parameters to be normally distributed *a priori* whereas "acc" indicates that the parameter values are assumed known. "CA" refers to the product of coverage areas. "WKNN" is the weighted 3-nearest neighbour method with the Euclidean distance.
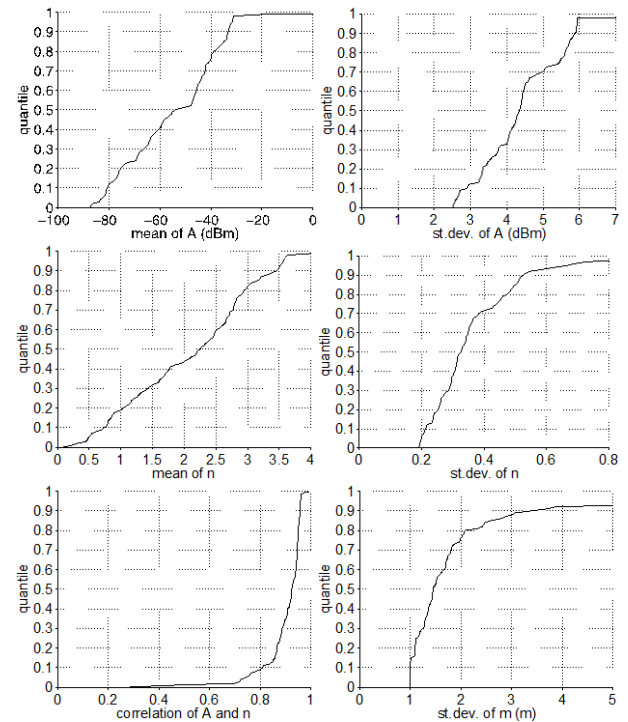

Figure 8: Estimate distributions for indoor WLAN APs: means of A (up left), standard deviations of A (up right), means of n (middle left), standard deviations of n (middle right), correlation coefficients of A and n (low left), and square-rooted maximal eigenvalues of the covariance matrices of m (low right).

Table 1: Results of static cellular positioning with real data

Solver	Mean (m)	Med (m)	95%err (m)	Cons (%)	Time (s)
Hervanta					
Grid, N	225	196	457	93	101
Grid, acc	227	219	460	81	54
MH, N	230	199	477	84	56
MH, acc	229	213	476	75	17
GN, N	209	190	451	94	0.7
GN, acc	219	200	480	72	0.6
CA	274	239	532	100	0.4
Lukonmäki					
Grid, N	203	149	495	93	105
Grid, acc	211	159	497	79	57
MH, N	215	156	562	84	74
MH, acc	224	165	543	73	24
GN, N	214	158	497	88	0.7
GN, acc	225	173	511	62	0.6
CA	248	195	548	95	0.4

Table 2: Results of cellular positioning with filter

Solver	Full learning data				Pruned learning data				Generic parameters, full learning data			
	Mean (m)	Med (m)	95%err (m)	Cons (%)	Mean (m)	Med (m)	95%err (m)	Cons (%)	Mean (m)	Med (m)	95%err (m)	Cons (%)
Hervanta												
Grid, N	192	174	385	81	209	202	394	78	250	235	548	64
Grid, acc	203	199	397	61	227	215	421	52	255	247	550	56
MH, N	196	186	391	64	209	201	401	61	259	233	615	44
MH, acc	208	210	398	47	232	213	438	43	274	250	606	40
GN, N	196	177	409	85	210	197	402	81	251	246	549	59
GN, acc	208	189	426	53	234	214	458	44	256	245	550	47
CA	223	178	496	85	295	311	536	72				
Lukonmäki												
Grid, N	179	142	444	80	165	125	504	78	182	146	499	75
Grid, acc	186	166	429	63	170	138	469	65	190	158	495	60
MH, N	187	145	494	65	169	124	527	68	191	150	532	65
MH, acc	194	165	433	51	182	148	468	52	197	167	491	53
GN, N	183	150	445	73	169	132	495	74	184	148	500	71
GN, acc	196	180	426	46	181	151	459	46	197	158	498	52
CA	210	188	486	84	207	158	559	78				

Table 3: Static outdoor positioning results with cell and WLAN in Lukonmäki

Solver	WLAN-CA				WLAN-CA&RSS				WLAN-RSS			
	Mean (m)	Med (m)	95%err (m)	Cons (%)	Mean (m)	Med (m)	95%err (m)	Cons (%)	Mean (m)	Med (m)	95%err (m)	Cons (%)
MH, N	82	41	318	25	82	43	316	25	122	65	403	90
MH, acc	83	39	345	26	80	42	323	25	115	70	399	80
GN, N	81	41	303	32	81	41	303	31	106	53	376	85
GN, acc	82	40	319	31	82	42	319	28	109	57	386	69
CA	84	42	318	34								

Table 4: Filtering results for the real data tests in the indoor case. WKNN not filtered.

Solver	Full learning data				Pruned learning data				Generic PL parameters, full learning data			
	Mean (m)	Med (m)	95%err (m)	Cons (%)	Mean (m)	Med (m)	95%err (m)	Cons (%)	Mean (m)	Med (m)	95%err (m)	Cons (%)
Grid, N	6.6	5.8	15.4	93	7.4	6.2	17.9	96	9.3	8.1	27.4	85
Grid, acc	6.6	5.6	15.6	80	7.0	5.2	18.7	82	8.7	7.1	28.5	71
MH, N	7.1	6.2	15.9	85	7.5	6.2	18.7	92	9.8	8.8	27.2	74
MH, acc	6.6	5.9	16.3	77	7.3	5.4	19.6	80	8.6	7.0	27.1	68
GN, N	6.7	6.0	15.5	93	8.4	6.4	22.9	82	9.3	6.7	29.4	80
GN, acc	7.1	6.2	15.3	60	8.8	6.9	24.3	51	9.5	6.2	32.1	58
CN	9.6	8.6	20.0	44	11.6	9.9	25.0	31	9.4	8.6	17.2	42
WKNN	4.5	3.2	10.5		9.5	8.4	17.6					

Table 5: Filtering results for the real data tests in the indoor case, positioning data being about 1.5 years newer than the learning data. WKNN not filtered.

Solver	Mean (m)	Med (m)	95%err (m)	Cons (%)
Grid, N	7.6	6.6	13.5	96
Grid, acc	7.5	6.1	13.9	90
MH, N	9.4	8.6	17.8	75
MH, acc	8.0	7.2	16.9	83
GN, N	7.6	6.7	15.6	92
GN, acc	6.8	6.4	15.3	82
CN	9.3	9.0	18.3	63
WKNN	8.3	4.9	31.4	

In terms of the error statistics presented in Table 4, the proposed RSS methods seem to perform better than the coverage area solution but worse than the WKNN solution in positioning accuracy. Note, however, that both Gauss–Newton solutions are computationally much more efficient and the requirements for the database are much lower for the parametric algorithms, since only the PL parameter estimates and their variances have to be stored for each AP instead of all the measurement points. Moreover, pruning the database seems to influence the fingerprint solution much more than the parametric methods; WKNN cannot interpolate the radiomap between the learning measurements like the physics-based statistical PL models. Based on the right column of Table 4, the generic parameters result in at least 20 % increase in the mean and median errors and in even larger differences in 95 % errors. According to aged radiomap results of Table 5, especially the WKNN method's performance suffers from the aged radiomap. By the low median error and large 95 % error, the performance of the WKNN is good most of the time with the aged radiomap, but deteriorates at certain areas.

The parameter uncertainties seem to be essential from the consistency's viewpoint also in the indoor case. In practice WLAN positioning in indoor spaces is complemented by additional, more refined sources such as map information, inertial navigation systems or Bluetooth. When several types of measurements are combined, it is crucial to be able to determine the accuracy of each measurement, and so the improvement in consistency is a good reason for taking the parameter uncertainties into account in indoor positioning.

8. Conclusions

This article presented statistical methods for dynamic path loss parameter estimation and positioning using received signal strength measurements. According to the tests performed using cellular and WLAN networks in outdoor spaces and WLAN networks in indoor spaces, RSS positioning based on dynamically estimated base station specific path loss parameters outperforms cell-

ID-based coverage area positioning and positioning with a generic path loss model. The accuracy is also comparable with the *k*-nearest neighbour method. The database requirements of path loss model methods are lighter than those of the *k*-nearest neighbour method, and the path loss model methods are less sensitive to inadequate database coverage and database aging. It was also shown that taking the parameter uncertainties into account in the positioning phase improves positioning accuracy and especially consistency of error estimates compared to the methods in which the path loss parameters are assumed accurately known. The differences are emphasized if some of the BSs have been estimated using a pruned learning database. Furthermore, it was shown that Gauss–Newton optimization algorithm provides satisfactory accuracy and consistency compared with grid and Metropolis–Hastings methods, being also computationally feasible for many real-time applications. Adding other sources of navigation information such as maps or inertia-based information and showing the influence of the parameter uncertainties in a hybrid positioning system in outdoor and indoor spaces is a topic for future research. Additional future topic is expanding the presented methods into 3D position space especially in indoor spaces, in which floor detection is an interesting and essential part of navigation.

References

[1] A. F. Molisch, *Wireless Communications,* 2nd ed. Wiley - IEEE, January 2011.

[2] T. S. Rappaport, *Wireless communications: Principles and practice, 2nd edition.* Prentice Hall PTR, 2008, ch. Mobile Radio Propagation: Large-Scale Path Loss.

[3] X. Li, "RSS-Based Location Estimation with Unknown Pathloss Model," *IEEE Transactions on Wireless Communications,* vol. 5, no. 12, pp. 3626–3633, December 2006.

[4] J. Rodas and C. J. Escudero, "Dynamic path-loss estimation using a particle filter," *IJCSI International Journal of Computer Science Issues,* vol. 7, no. 4, May 2010.

[5] A. Bose and C. H. Foh, "A practical path loss model for indoor WiFi positioning enhancement," in *6th International Conference on Information, Communications Signal Processing, 2007,* December 2007.

[6] S. Mazuelas, F. A. Lago, D. González, A. Bahillo, J. Blas, P. Fernandez, R. M. Lorenzo, and E. J. Abril, "Dynamic estimation of optimum path loss model in a RSS positioning," in *Position, Location and Navigation Symposium, 2008 IEEE/ION,* May 2008, pp. 679–684.

[7] H. Nurminen, J. Talvitie, S. Ali-Löytty, P. Müller, E.-S. Lohan, R. Piché, and M. Renfors, "Statistical path loss parameter estimation and positioning using RSS measurements," in *Ubiquitous Positioning Indoor Navigation and Location Based Service (UPINLBS2012),* October 2012, pp. 1–8.

[8] H. Nurminen, J. Talvitie, S. Ali-Löytty, P. Müller, E.-S. Lohan, R. Piché, and M. Renfors, "Statistical path loss parameter estimation and positioning using RSS measurements in indoor wireless networks," in *2012 International Conference on Indoor Positioning and Indoor Navigation (IPIN2012),* November 2012, pp. 1–9.

[9] M. Hata, "Empirical formula for propagation loss in land mobile radio services," *IEEE Transactions on Vehicular Technology,* vol. VT-29, no. 3, pp. 317–325, 8 1980.

[10] M. Gudmundson, "Correlation model for shadow fading in mobile radio systems," *Electronics Letters,* vol. 27, no. 23, pp. 2145–2146, November 1991.

[11] S. Shrestha, E. Laitinen, J. Talvitie, and E. S. Lohan, "RSSI channel effects in cellular and WLAN positioning," in *9th Workshop on Positioning, Navigation and Communication 2012 (WPNC' 12),* March 2012.

[12] J. S. Liu, *Monte Carlo Strategies in Scientific Computing.* Springer, 2001.

[13] N. Sirola, "Closed-form algorithms in mobile positioning: Myths and misconceptions," in *7th Workshop on Positioning, Navigation and Communication 2010 (WPNC'10),* Dresden Germany, March 2010, pp. 38–44.

[14] Å. Björck, *Numerical methods for least squares problems.* Society for Industrial and Applied Mathematics, 1996.

[15] A. Ruhe, "Accelerated Gauss-Newton algorithms for nonlinear least squares problems," *BIT Numerical Mathematics,* vol. 19, no. 3, pp. 356–367, 1979.

[16] L. Koski, T. Perälä, and R. Piché, "Indoor positioning using WLAN coverage area estimates," in *2010 International Conference on Indoor Positioning and Indoor Navigation (IPIN2010),* September 2010.

[17] L. Koski, R. Piché, V. Kaseva, S. Ali-Löytty, and M. Hännikäinen, "Positioning with coverage area estimates generated from location fingerprints," in *7th Workshop on Positioning, Navigation and Communication 2010 (WPNC'10),* March 2010, pp. 99–106.

[18] V. Honkavirta, T. Perälä, S. Ali-Löytty, and R. Piché, "A Comparative Survey of WLAN Location Fingerprinting Methods," in *6th Workshop on Positioning, Navigation and Communication 2009 (WPNC' 09),* 2009, pp. 243–251.

[19] Y. Bar-Shalom, R. X. Li, and T. Kirubarajan, *Estimation with Applications to Tracking and Navigation, Theory Algorithms and Software.* John Wiley & Sons, 2001.

[20] S. Ali-Löytty, N. Sirola, and R. Piché, "Consistency of three Kalman filter extensions in hybrid navigation," in *The European Navigation Conference GNSS 2005,* Munich, Germany, July 2005.

[21] B. Ristic, S. Arulampalam, and N. Gordon, *Beyond the Kalman Filter, Particle Filters for Tracking Applications.* Boston, London: Artech House, 2004.

Biography

Henri Nurminen is a PhD student in the Department of Automation Science and Engineering at Tampere University of Technology, Finland. He received his MSc degree from the same university in 2012. His research interests are Bayesian filters and Monte Carlo estimation in personal indoor and outdoor positioning with signals of opportunity.